Elastic waves push organic fluids from reservoir rock

Igor A. Beresnev,[1] R. Dennis Vigil,[2] Wenqing Li,[2] Wayne D. Pennington,[3]
Roger M. Turpening,[3] Pavel P. Iassonov,[1] and Robert P. Ewing[4]

Received 31 March 2005; revised 9 May 2005; accepted 26 May 2005; published 6 July 2005.

[1] Elastic waves have been observed to increase productivity of oil wells, although the reason for the vibratory mobilization of the residual organic fluids has remained unclear. Residual oil is entrapped as ganglia in pore constrictions because of resisting capillary forces. An external pressure gradient exceeding an ''unplugging'' threshold is needed to carry the ganglia through. The vibrations help overcome this resistance by adding an oscillatory inertial forcing to the external gradient; when the vibratory forcing acts along the gradient and the threshold is exceeded, instant ''unplugging'' occurs. The mobilization effect is proportional to the amplitude and inversely proportional to the frequency of vibrations. We observe this dependence in a laboratory experiment, in which residual saturation is created in a glass micromodel, and mobilization of the dyed organic ganglia is monitored using digital photography. We also directly demonstrate the release of an entrapped ganglion by vibrations in a computational fluid-dynamics simulation. **Citation:** Beresnev, I. A., R. D. Vigil, W. Li, W. D. Pennington, R. M. Turpening, P. P. Iassonov, and R. P. Ewing (2005), Elastic waves push organic fluids from reservoir rock, *Geophys. Res. Lett.*, *32*, L13303, doi:10.1029/2005GL023123.

1. The Problem

[2] Elastic waves and earthquakes have been known to increase output of oil wells. Miscellaneous observations of this phenomenon have been summarized by *Beresnev and Johnson* [1994]. Empirical evidence has been strong enough to suggest sonication of reservoirs as a method of enhanced petroleum recovery (see review by Beresnev and Johnson for a history of applications; also, *Hilpert et al.* [2000], *Roberts et al.* [2001], and *Poesio et al.* [2002]). The development of sonic (vibratory) methods of enhancing reservoir yields has nevertheless not kept pace with the progress in its theoretical understanding. Nearly a dozen various physical mechanisms, which could potentially lead to enhanced percolation of organic fluids in porous rock subjected to vibrations, were proposed in the literature, none of which being satisfactory in its explanation of how weak, low-frequency perturbations could mobilize the droplets of residual oil causing them to move in unilateral direction.

[1]Department of Geological and Atmospheric Sciences, Iowa State University, Ames, Iowa, USA.
[2]Department of Chemical Engineering, Iowa State University, Ames, Iowa, USA.
[3]Department of Geological and Mining Engineering and Sciences, Michigan Technological University, Houghton, Michigan, USA.
[4]Department of Agronomy, Iowa State University, Ames, Iowa, USA.

0094-8276/05/2005GL023123$05.00

[3] To better understand the reason why the elastic waves can mobilize residual organic fluids, one should recall why these fluids are trapped. The primary reason for the entrapment is capillary forces, which arise from differences in the diameters of pore channels through which the organic fluids are driven by external pressure gradients. The mechanism of the entrapment is illustrated in Figure 1, which assumes a typical water-flooded reservoir in which an externally created pressure gradient pushes the fluids toward the producing well; the residual oil has been formed as isolated pools or ganglia [e. g., *Payatakes*, 1982]. Assuming oil as a non-wetting phase, an excess capillary pressure builds up on the internal side of the downstream meniscus entering the pore constriction, according to the Laplace equation, $P_c^{right} = 2\sigma/R^{right}$, where σ is the oil/water interfacial tension, and R^{right} is the radius of the right meniscus. Because the radius of the left meniscus R^{left} is greater, an internal capillary-pressure imbalance is created, resisting the external gradient (shown as an opposing arrow inside the blob in Figure 1); when this imbalance equals the driving external pressure difference ΔP, the ganglion stops. To carry it through, the external gradient needs to exceed a certain ''unplugging'' threshold ∇P_0. Sketching the flow rate as a function of the external gradient, we obtain a diagram shown as a solid line in Figure 2. The flow rate is zero (the ''no-flow'' zone in the diagram) until the value of the current static gradient ∇P_s exceeds ∇P_0, at which point the flow starts to follow the normal Darcy law (the ''flow'' zone).

[4] Had it not been for the action of capillary forces, all oil would have eventually been recovered. It has been suggested therefore that the mechanism of vibratory mobilization of the ganglia entrapped in pore constrictions should be sought in the effects of vibrations on capillary forces [*Graham and Higdon*, 2000a, 2000b; *Iassonov and Beresnev*, 2003].

2. Mechanism of Vibratory Mobilization of Entrapped Organic Ganglia

[5] Assume the system in Figure 1 is residing under a static gradient ∇P_s that is below the unplugging threshold ∇P_0, and then the longitudinal vibration of the wall is applied (without loss of generality, we consider the wall motion parallel to the pore axis). This motion induces an inertial forcing P_{osc} on the fluid with the amplitude of approximately $\rho_f a_0$, where ρ_f is the density of the fluid and a_0 is the amplitude of the acceleration of the wall [e.g., *Biot*, 1956, equation 2.4]. One cycle of this forcing, oscillating around the static value ∇P_s, is shown on a vertical scale in Figure 2. The instant total forcing on the fluid thus becomes $P_{\mathrm{osc}} + \nabla P_s$. In the positive half-period of vibrations, when the total forcing exceeds ∇P_0, the ganglion is instantly ''unplugged'' and moves forward, whereas, when

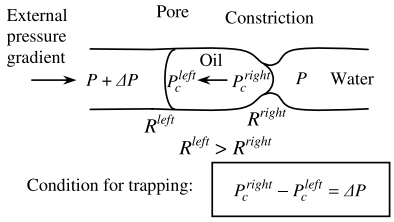

Figure 1. Organic-ganglion flow through a constricted pore under the effect of external pressure difference ΔP. R^{left} and R^{right} are the radii of the left and the right menisci, respectively. The ganglion is trapped when the condition in the box is satisfied.

the vibration reverses direction, the flow is plugged. A "rectification" effect takes place, leading to a "nudging" motion of the ganglion through the constriction during the positive half-cycles. After a number of cycles, the ganglion is mobilized.

[6] Once the ganglion is unplugged and starts moving, the radius of its right meniscus is progressively increased, leading to the decrease in the resisting capillary force as the motion continues. As a result, the total forcing acting on the ganglion during the positive half-cycle grows over time, causing the ganglion to accelerate upon exiting the constriction. This acceleration creates a nonlinear dependence of the blob's distance traveled on the time spent in the unplugged position, and consequently the non-equivalence of the vibrations applied at different frequencies.

[7] Note that the operation of the mechanism discussed only requires the presence of the longitudinal vibrations of the wall, which could be created by either conventional *P*-wave or conventional *S*-wave; the presence of any other types of waves, including the Biot slow wave, is not required.

[8] Two specific predictions can be made based on this mobilization phenomenon. For a fixed frequency, the enhancement in the ganglion flow will grow with increasing acceleration amplitude of vibrations, which will simply increase the amplitude of P_{osc}. For a fixed amplitude, the effect will be inversely proportional to the frequency, which can be expected for two reasons. First, in order to be unplugged, the ganglion needs to be moved to the narrowest point in the constriction over one period of vibrations, which can only be achieved if the frequency is low enough. Second, the displacement of the ganglion over one period will depend on how much time it spends in the unplugged position. Higher frequencies will result in a smaller cumulative forward motion because of the ganglion acceleration effect: a greater displacement is achieved at one longer period than at a number of shorter periods even if they add up to the same total "unplugged" duration.

[9] The predictions of the amplitude and frequency dependence of the mobilized flow can be directly verified by experiment.

3. Experimental Observation of the Mobilization Effect

[10] An experimental apparatus was built to directly observe the vibratory mobilization of entrapped organic ganglia. A 50 × 50 square lattice of circular pore bodies connected by straight pore throats was etched onto two glass plates, and the plates were annealed together. The body and throat diameters were normally distributed and had mean values of 2.30 and 0.76 mm, with a distance of 3.80 mm between the centers of neighbor bodies. The etching depth was approximately 0.1 mm. The total volume of the voids (pore bodies + throats) was 3.2 cm^3, with a porosity of 0.44. The length of the lattice was 19 cm.

[11] This horizontally mounted micromodel was filled with trichloroethylene (TCE), a common organic solvent having negligible solubility in water. The TCE was then displaced by degassed water under a constant-pressure drop of 700 Pa between the inlet and outlet, until a residual saturation was reached. Catalytic amounts of organic dye (Oil Blue N) were added to the organic fluid to enable its visualization by photography. Digital photographs were taken, and image-analysis software was used to calculate the fractional area of void space occupied by the dye-containing TCE. This allowed us to monitor the evolution of the two-phase system over time under the conditions of water flood.

[12] The flow experiment was conducted both without vibrations and with vibrations applied to the micromodel at various amplitudes and frequencies. Vibrations were applied horizontally using an exciter along the axis connecting the inlet and the outlet. The frequency and amplitude of acceleration were controlled by a function generator and amplifier. An accelerometer was placed on the micromodel

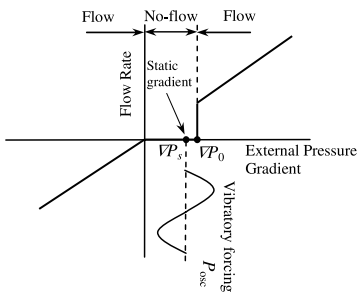

Figure 2. The mechanism of the "nudged" release of the ganglion from its trapped position under the combined effect of external gradient and vibrations.

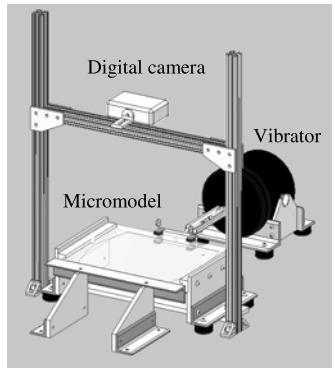

Figure 3. Sketch of the experimental set-up.

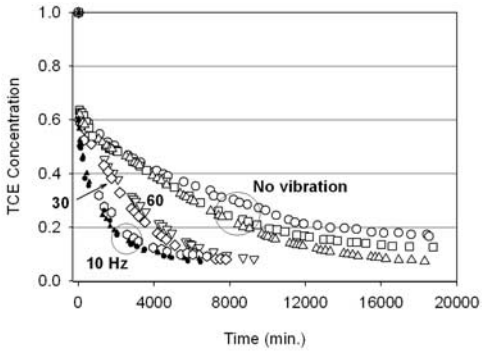

Figure 4. Concentration of TCE displaced by water as a function of time. The effect of vibration at different frequencies is shown, at a constant acceleration amplitude of 3.5 m/sec^2.

to measure the acceleration. A sketch of the experimental set-up is shown in Figure 3.

[13] From the general form of the Laplace equation for non-spherical menisci, the maximum difference in capillary pressure along a ganglion trapped in the micromodel is estimated as $\Delta P_c = \sigma(1/R^{right} - 1/R^{left})$, where R^{right} and R^{left} are the radii of the pore throat and body in the micromodel, respectively. Using the mean values of R^{right} = 0.38 mm and R^{left} = 1.15 mm, σ for TCE/water interface of 0.035 N/m, we obtain $\Delta P_c \approx 62$ Pa. Considering a typical length of entrapped TCE ganglia of about four inter-body distances, the capillary body force keeping the ganglia in place is estimated as $\Delta P_c/\Delta x \approx 62$ Pa/(4 $\times$ 0.0038 m) = 4.1 $\times$ 10^3 N/m^3. On the other hand, the body force exerted on the ganglia by the pressure drop along the model is 700 Pa/0.19 m = 3.7 $\times$ 10^3 N/m^3. This body force was thus on average below the capillary force resisting it, explaining favorable conditions for trapping. Under these conditions, an acceleration of the micromodel of 2.5 m/sec^2 would create an oscillatory body force of $\rho_f a_0$ = 3.7 $\times$ 10^3 N/m^3, equal to the external gradient (based upon the TCE density of 1462 kg/m^3). This would double the peak total external forcing acting on the fluid, which would thereby exceed the resisting capillary body force. This initial estimate provided us with a range of accelerations that could allow observation of the mobilization effect.

[14] Figure 4 illustrates the effect of the frequency of vibrations on TCE concentration as a function of time, at fixed acceleration amplitude of 3.5 m/sec^2. We first conducted three runs of the experiment without vibrations to check the repeatability of the results and establish a natural scatter in residual concentrations (three encircled upper curves in Figure 4). The experiment then was repeated with the vibrations applied from the beginning of TCE displacement by water, at frequencies of 10, 30, and 60 Hz. The experiment at 10 Hz was conducted three times to again check the reproducibility (three encircled lower curves). As Figure 4 shows, an inverse dependence of TCE removal on frequency was observed, as anticipated, with the highest rate of TCE production at the lowest frequency of 10 Hz.

[15] The experiment was then carried out to address the amplitude effect on the TCE production at a constant vibration frequency of 30 Hz. The displacement was first conducted with no vibrations applied, and then with vibrations on from the beginning with acceleration amplitudes of 0.5, 1.75, 3.5, and 7.5 m/sec^2 (Figure 5). The mobilization effect grew with the amplitude, with the highest rate of TCE removal at the largest acceleration amplitude of 7.5 m/sec^2.

[16] These experimental results obtained in a controlled environment, in which we could directly observe the formation and mobilization of residual organic ganglia, confirm the principal predictions of the mechanism of mobilization by elastic waves and vibrations. The increase in the rate of TCE production proportional to the amplitude and inversely proportional to the frequency is explained by the vibrations preventing the entrapment: the ganglia that would have been entrapped without vibrations are able to overcome the capillary barrier when the system undergoes vibration due to the nudging effect. The amount of entrapped organic phase is thus lower at any given time than if there were no vibrations. The vibrations are aiding the unrestricted motion of the organic phase.

4. Numerical Simulation of Ganglion Release by Vibrations

[17] The release of an entrapped organic ganglion by the application of elastic-wave motion of the wall can also be demonstrated by a direct numerical experiment. In carrying out this simulation, we used the finite-volume computational-fluid-dynamics software FLUENT. A TCE ganglion suspended in water in an axisymmetric constricted pore channel was placed upstream of a constriction and freely displaced by an external pressure gradient until it became entrapped at the entrance to the constriction. Figure 6a shows the computational domain with the entrapped ganglion; the initial motion was from left to right. The constant pressure difference between the left and the right sides of the domain was set at 30 Pa.

[18] Similar numerical experiments were conducted by *Graham and Higdon* [2000b], which however lacked in their practical relevance, i. e., did not answer the question of whether the vibratory mobilization was theoretically feasible for realistic porous media and the fields that could penetrate them. Also, all principal results of the study were

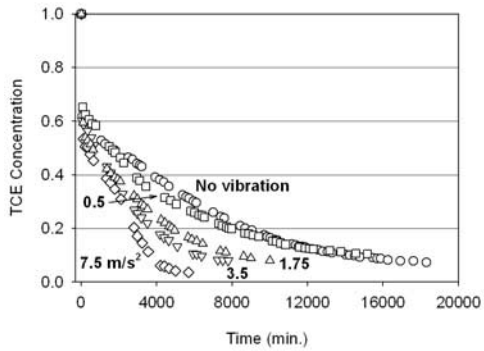

Figure 5. Concentration of TCE as a function of time. The effect of vibration with different acceleration amplitudes is shown, at a constant frequency of 30 Hz.

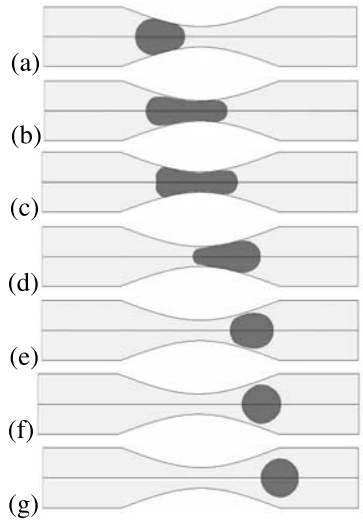

Figure 6. Numerical simulation of the organic-ganglion mobilization by vibrations of the wall. Snapshots are made at 0.0, 0.025, 0.050, 0.075, 0.100, 0.125, and 0.150 sec (a–g, respectively) after the vibrations were turned on; (a) corresponds to the initial entrapped configuration.

obtained for the zero material-property number $\rho_f \sigma R/\mu^2$, where R is the minimum radius of the constriction and μ is the fluid dynamic viscosity. Clearly, this number can only be zero for the zero interfacial tension, implying there was no capillary entrapment that the authors sought to describe. This makes the results difficult to interpret, while our simulations do not suffer from this contradiction.

[19] In all simulations, the mesh-generation software GAMBIT was used to construct the 40 (radial) $\times$ 160 (axial) grid, on which the unsteady continuity, momentum, and volume fraction equations were solved. Grid spacing was non-uniformly distributed to provide finer resolution near the walls. Simulations used the second-order space-differencing and first-order implicit time-differencing schemes. Grid refinement studies were performed to ensure that the computed solutions were grid-independent. The TCE/solid contact angle was set at 170°. Diameters of the channel, the narrowest (middle) section of the constriction, and the original undeformed ganglion were 3, 1, and 2 mm, respectively. The length of the computational domain was 16 mm. Each complete simulation took approximately 12 hours on a Dell 2.4 GHz Pentium-4 workstation.

[20] The ganglion in Figure 6a is unable to flow due to the capillary barrier. Figures 6b–6g show snapshots of the problem domain at uniform time increments of half the vibration period after wall vibrations at 20 Hz and an acceleration amplitude of 19 m/sec^2 were turned on (a complete movie is available upon request). In this experiment, the ganglion becomes mobilized after the second cycle (Figure 6e). Perusal of the complete movie shows the ganglion slightly retreating into the constriction during the negative half of the first cycle, followed by its total release. The only factor responsible for the mobilization is the elastic-wave motion of the wall, in accordance with the expectation from the mechanism. We performed further numerical experiments for various frequency-amplitude combinations and observed a decrease in the acceleration amplitude needed to mobilize the flow with decreasing frequency. This also naturally follows from the mechanism. Since, for the ganglion to be mobilized, it needs to be brought to the narrowest point in the constriction over one period, as period increases, the driving forcing can decrease and still satisfy this condition.

5. Implications

[21] Each individual residual ganglion in each pore resides in equilibrium with the external pressure gradient and is characterized by its individual total-forcing threshold required for mobilization. This capillarity-controlled threshold in natural media will be dependent on oil/water interfacial tension, the geometry of the throat, and the properties of the solid (through the contact angle), and will thus be different from one pore to another. The vibrations, by adding to the constant gradient, "unplug" the ganglia for which the threshold is exceeded, leaving others intact. An elastic wave of a given amplitude and frequency will thus *always* produce a certain mobilization effect, "picking out" the ganglia favoring mobilization and leaving others unaffected. The percentage of mobilized oil will grow with larger amplitudes and lower frequencies.

[22] *Graham and Higdon* [2000a] argue that non-sinusoidal vibratory waveforms can achieve greater ganglion-flow enhancement in straight channels. They suggest a spike wave, consisting of brief periods of positive forcing separated by longer low "plateaus" of forcing in the negative direction [*Graham and Higdon*, 2000a, Figure 11]. The same effect will be achieved in the release of the ganglia from narrow constrictions, but for a different reason. As follows from the mechanism in Figure 2, the mobilization occurs due to the forcing in the positive direction. A hypothetical "rectified" sinusoidal wave consisting of positive half-periods separated by plateaus will thus be more efficient than a pure sinusoidal wave with the same frequency.

[23] The chief difference between the elastic-wave mobilization of residual oil and the other enhanced-recovery methods is in the means of delivering the mobilizing energy. The traditional methods, which utilize hydraulic paths to supply additional forcing to the trapped ganglia, suffer from bypassing effects, in which the agents flow with water along preferential paths of least resistance, leaving hydrologically isolated oil pools untapped. In contrast, seismic energy has no preferential path and reaches every point of the porous space.

[24] **Acknowledgments.** This work was supported by the National Science Foundation award EAR-0125214 and Department of Energy award DE-FC26-01BC15165. We are indebted to two anonymous reviewers for providing helpful comments.

References

Beresnev, I. A., and P. A. Johnson (1994), Elastic-stimulation of oil production: A review of methods and results, *Geophysics*, *59*, 1000–1017.

Biot, M. A. (1956), Theory of propagation of elastic waves in a fluid-saturated porous solid. II. Higher frequency range, *J. Acoust. Soc. Am.*, *28*, 179–191.

Graham, D. R., and J. J. L. Higdon (2000a), Oscillatory flow of droplets in capillary tubes. Part 1. Straight tubes, *J. Fluid Mech.*, *425*, 31–53.

Graham, D. R., and J. J. L. Higdon (2000b), Oscillatory flow of droplets in capillary tubes. Part 2. Constricted tubes, *J. Fluid Mech.*, *425*, 55–77.

Hilpert, M., G. H. Jirka, and E. J. Plate (2000), Capillarity-induced resonance of oil blobs in capillary tubes and porous media, *Geophysics*, *65*, 874–883.

Iassonov, P. P., and I. A. Beresnev (2003), A model for enhanced fluid percolation in porous media by application of low-frequency elastic waves, *J. Geophys. Res.*, *108*(B3), 2138, doi:10.1029/2001JB000683.

Payatakes, A. C. (1982), Dynamics of oil ganglia during immiscible displacement in water-wet porous media, *Annu. Rev. Fluid Mech.*, *14*, 365–393.

Poesio, P., G. Ooms, S. Barake, and F. van der Bas (2002), An investigation of the influence of acoustic waves on the liquid flow through a porous material, *J. Acoust. Soc. Am.*, *111*, 2019–2025.

Roberts, P. M., A. Sharma, V. Uddameri, M. Monagle, D. E. Dale, and L. K. Steck (2001), Enhanced DNAPL transport in a sand core during dynamic stress stimulation, *Environ. Eng. Sci.*, *18*, 67–79.

I. A. Beresnev and P. P. Iassonov, Department of Geological and Atmospheric Sciences, Iowa State University, 253 Science I, Ames, IA 50011-3212, USA. (beresnev@iastate.edu)

R. P. Ewing, Department of Agronomy, Iowa State University, 2101 Agronomy Hall, Ames, IA 50011-1010, USA.

W. Li and R. D. Vigil, Department of Chemical Engineering, Iowa State University, 2114 Sweeney Hall, Ames, IA 50011-2230, USA.

W. D. Pennington and R. M. Turpening, Department of Geological and Mining Engineering and Sciences, Michigan Technological University, 1400 Townsend Dr., Houghton, MI 49931, USA.